

Design and Simulation of an Optimized Mixed Mode Solar Dryer Integrated With Desiccant Material

Ahmed Alqadhi, S. Misha, M.A.M.Rosli, and M.Z.Akop

Abstract— Solar drying is one of the methods that have been used since ancient times. This system has been constantly developed in the last few years to acquire better effective results and drying performance. The efficiency of the solar dryer is essentially depends on the thermal distribution and uniformity of flow inside the dryer body. In this paper, a conceptual design of a mixed mode solar dryer which includes direct and forced indirect solar drying integrated with desiccant materials is developed and proposed. Some concepts of this design are new and others are inspired from recent works. Based on these, this mixed mode solar dryer is prospective to be superior in the rate of drying as well as air flow uniformity. Moreover, this improved drier which can be utilized for drying the diverse agricultural products is a simple system and might be manufactured locally. In addition, a simulation of the system using CFD (Computational Fluid Dynamic) software was performed for the optimization of drying chamber configuration by predicting the airflow distribution, temperature and velocity profiles throughout the dryer. This simulation process has the capability to resolve equations of mass conversation, energy and momentum utilizing numerical approach and it is a very useful tool to evaluate the temperature and velocity profiles in the various positions of the system and attain a uniform air flow with higher temperature inside drying cell or chamber. Simulation results are suitable for further validation against an experimental results of the same design.

Index Term— Solar dryer, Mixed mode solar drying, CFD Simulation, Drying chamber

I. INTRODUCTION

DRYING can be defined as the process of removing water or other liquids by evaporating from products. It is an ancient method that utilizes solar energy to dry an object, in which the object is exposed to the sun radiation so that it can be evaporated [1]. Usually, drying is the simple and final step in production, which includes removal of the moisture contents from a product prior to packaging and presenting it to the market. Drying products by exposing them to the sun energy can be economic techniques since it reduces the cost of drying operation in comparison to the conventional drying machineries. In contrast, this method has many drawbacks including products spoiling due to rainy weather, winds, moistures and dusts. Also, possibility of product damage can

occur due to animals, birds or any other objects hitting the products. Based on these, solar drying technology can be a promising system to be utilized as drying method. Solar drying system can save energy, consume less time, utilize less space, enhance the product quality, increase the efficiency of the process and save the environment [2]. Therefore, we must consider developing such renewable energy resources which have less impact to the environments as well as can be produced at less costs [3]. Several of dryers were utilized in the home and industrial fields. The dryers which are well-known are tray dryers, tunnel dryers, drum dryers, and many more. Within all these types, the tray dryer is the most extremely utilized due to its simplicity and less cost construction [4].

Solar dryer systems can be categorized into three different classes which are direct, indirect and mixed mode in accordance to the passive mode of drying process. The crucial feature of the solar drying system can be visualized from the fact that they operate fully with renewable energy which environmentally friendly and free of pollution. The construction of solar dryer system can be achieved simply with an existed materials. In this study, the type of solar dryer is called mixed mode, which combining both direct and indirect drying methods in which the hot air coming from the separated solar cell is transferred forcibly by fans as well as naturally to the drying chamber. The advantages of such drying methods are having less humidity content and higher drying rate in comparison to other relative methods [5].

In contrast, there are some items which cannot be dried at high thermal rate such as foods, curative and other thermal susceptible products. The reason behind this is the possibility of affecting the product quality or damaging them. Therefore, suitable desiccant materials need to be used in the drying process which can absorb the humidity from the air. A moisture removal process produces not just dried air, but rise up thermal rate, because of the isothermal operation. At low thermal or during the off-sunshine times at night, the drying process can be achieved by utilizing a material that can keep the color of the product [6]. The implementation of desiccants is accounted as renewable energy, but the regenerating operation can be achieved by renewable or non-renewable energy. Desiccants are combined elements, like montmorillonite clay, silica gel,

¹This work was supported and funded by Universiti Teknikal Malaysia Melaka (UTeM) for research grant PSP/2016/FKM-Care/S01507.

* Ahmed Alqadhi, #S.Misha, M.A.M.Rosli, and M.Z.Akop are with the Faculty of Mechanical Engineering, Universiti Teknikal Malaysia Melaka

(UTeM), 76100 Durian Tunggal, Melaka, Malaysia (e-mail: *alqadhi2011@gmail.com, #suhaimimisha@utem.edu.my).

molecular sieve, calcium sulfate and calcium oxide [7].

Employing an efficient designing of a tray dryer can contribute to reduce the low air diffusion in the dryer cell. Usually, conducting a measure of the drying product is expensive, hard to achieve, and require long time because of the big number of sensors and logging data devices required to be attached in various area of the drying system. This can be very expensive, especially when dealing with high-volume drying process [8]. Nowadays, a new simulation approach called Computational Fluid Dynamics (CFD) which has the capability to resolve equations of mass conversation, energy and momentum utilizing numerical approach. This can help to anticipate the thermal rate, velocities and pressure of the drying cell or chamber.

Mathioulakis et al. [9], developed and built an industry based tray dryer to dry fruits. CFD is employed in order to simulate the air stress profiles and air speed distributing in dryer cell. The outcomes indicate that a difference in the last humidity value occurred in many trays; also irregularity existed within certain areas of the cell. An extremely correlating relationship between the dryer rate and air speed is noticed by comparing the simulated results of CFD with the experimental data.

Dionissios and Adrian-Gabriel Ghious [10], investigated a numerical simulation within a drying chamber with big number of trays. In order to validate the model, a number of experimental measures have been accomplished on a single tray. The standardized K-e model proved to be the most sufficient model based on the comparison between the simulation results of CFD and measurement data.

Jacek Smolka et al. [11], discussed a numerical system of a dryer oven utilizing the CFD simulating approach. The obtained data indicates god agreement with the experimental results. Many novel models were employed to enhance irregularity of thermal rate within the e chamber. A different form and location of the heaters and baffles controlling the air flowing were considered as the best sufficient.

In this paper, the main aim of the design is to obtain the most possible uniform flow in parallel with achieving a high temperature by the solar panels. In another meaning, we are not seeking for the highest temperature gained only, but both the two important parameters which are the air uniformity and high temperature. If these two parameters have fulfilled perfectly, then the best drying rate could be achieved. Therefore, this design of the mixed mode solar dryer is developed and optimized up to a certain level that the drying rate could be reduced significantly taking in consideration the quality of product.

II. DESIGN OF THE SYSTEM

The design of the product is conducted using solid work software, this design combines all the diverse modes of drying, direct, indirect, and silica gel materials that used to absorb the moisture during the night and off sun times. It has diverse modifications and enhancements which makes it distinct from the previous designs .Some of these modifications are new concepts and others are inspired from the previous designs. These amendments had been applied to this design to

ameliorate the performance and help to acquire better results of drying process with the consideration of the quality of products. The first new concept in this design is that the solar air cell including the solar plates absorbers are attached to the drying chamber from two sides instead of one side in order to increase the temperature achieved by chamber and therefore increasing the efficiency of the system as well .Furthermore, a special advantage of this design is that it has a recirculate pipe from the exit of the chamber and returns back to the bottom inlet of the chamber. Moreover, two speeding fans are located at the bottom of the chamber above the bottom inlet of the air to get better air flow and circulation inside the chamber. The configuration of this mixed mode solar dryer is presented in Fig. 1.

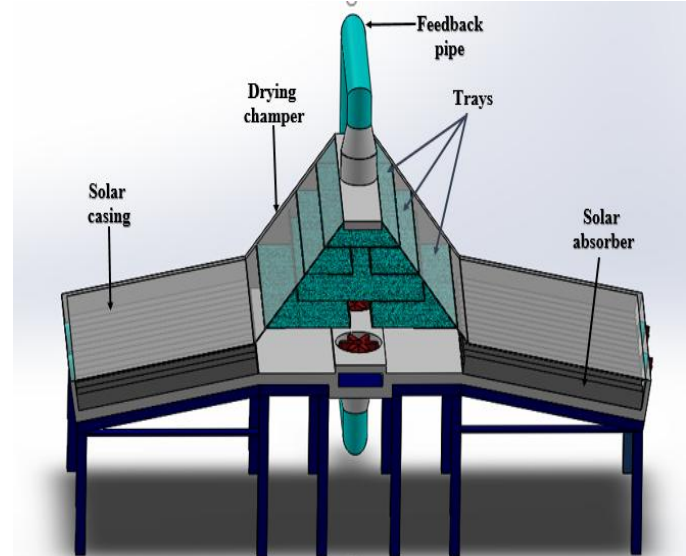


Fig. 1. Configuration of the designed system.

As it can be seen from the figure above, there are four main parts implemented in this design as follow:

A. Air solar heaters.

There are two air solar absorber attached to both sides of the drying chamber .These solar panels are implemented to rise up the temperature inside the solar casing by absorbing the heat directly from sun radians [12].The dimensions of the casing of the solar panels are 80 cm long, 84 width, and 15 cm height .Inside the casing, an insulation of 2 cm thickness is placed at the sides of the air solar casing. However, at the bottom of the casing, the insulation thickness is higher than that on the sides because of the high temperature transferred by the solar panels. Therefore, its thickness intended to be 4 cm as shown in the Fig. 2.The function of the insulation is to maintain the high gained temperature inside the dryer for longer time and avoid the leakage of heat .The panels are placed inclined to the horizontal plane by 10 degree [13]. This is calculated regarding the location of the UTeM university in Malaysia which lies on Latitude and longitude coordinates of: 2.200844 N, 102.240143E respectively [14]. This inclination is to position the sun radiation perpendicular to the solar panels and achieve the most possible heat from the sun. The panels are then placed on the top of the back insulation .The aluminum panels are shaped in V Groove shape with 60 degree angle and maintained

inside the solar casing as shown in the Fig.2.

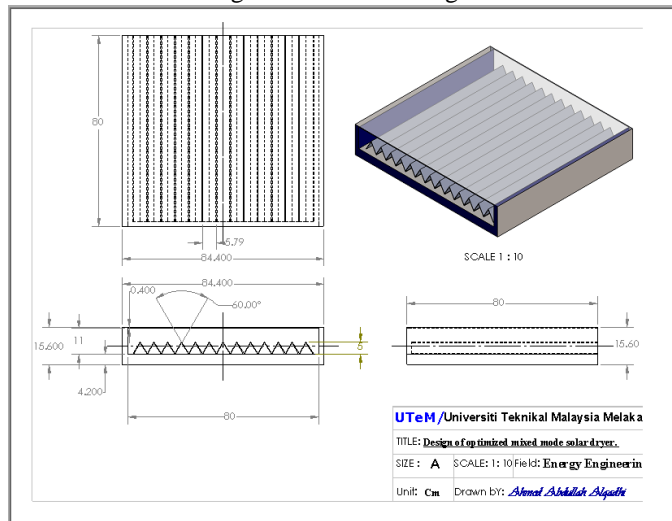


Fig. 2. V groove solar collector.

V-groove shape increase the surface area of the absorbers and thus increase the total amount of radiations falls onto solar panels. Based on these, it leads to gain higher temperature inside the casing from radiations [15]. The upper surface of the casing made up from Glass with 4 mm thickness and permissively of 95 %, allowing higher amount of radiations to pass to the panels. Two controlled speed fans of 10 cm diameter are positioned in each side of solar panel casings (Fig. 3) to force the air towards the drying chamber with higher velocity and two fans at the bottom of the chamber with 20 cm diameter to distribute the air to all directions of the chamber. The process of forced air is recognized as forced indirect solar drying. In this part of the system a uniform air flow inside the solar panel cell is going to be achieved.

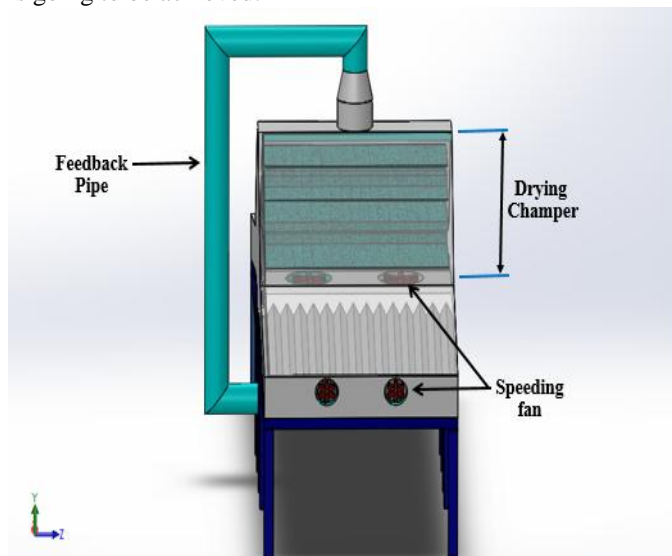


Fig. 3. Isometric view of fans and feedback pipe.

B. Drying chamber.

The drying chamber is the container where the product is placed and dried. The chamber is located between the two solar panels and it is perpendicular to the horizontal plane. This drying chamber integrates a mixed mode system to receive heat

in two methods, direct and indirect method. In the first mode which is indirect mode, it receives the heated air coming out from the solar collector and speeded up with fans [16]. While in the second mode, which is the direct method, the radiant heat is absorbed directly through the transparent side walls of the chamber which made up from glasses. Inside the chamber, layers of stationary trays are fixed in a different format to provide better air distribution through the trays [17]. The height of the first layer above the bottom surface is 20 cm, then the remaining trays are arranged with an equal height from each other with a value of 10 cm .Fig. 4 displays all the dimensions and details of the design in three projections, front, side, and top view.

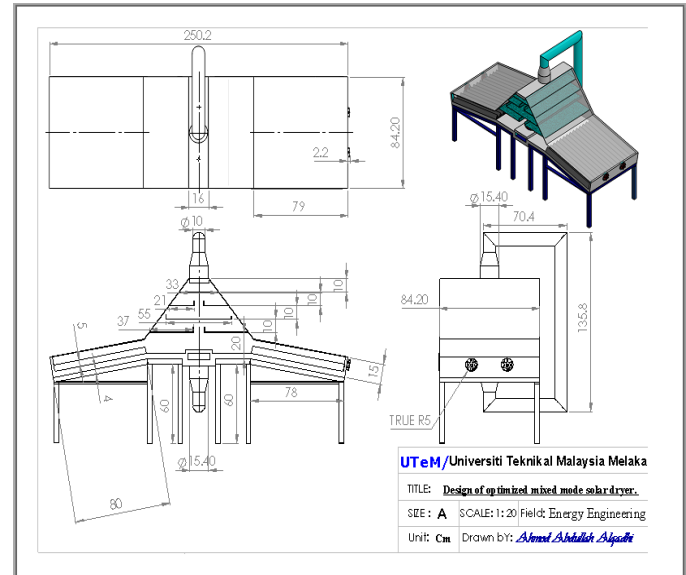


Fig. 4. Detailed dimensions of the design.

A desiccant materials are aimed to be placed beneath the first lower tray during the off sunshine .On the bottom surface of the chamber, two blowing fans are installed in order to speed up the hot air entering the chamber from the solar collectors. On the other hand, an exhaust fan is installed at the top to release the dehumidified air out of the drying chamber. During hot weather, drying of the products is held by the high temperature air inside the chamber while during the off sunshine, the system is supported by a desiccant materials to remove the moisture in a continuous drying process [18] .

C. Recirculate pipe.

The recirculate pipe is connected between the outlet of the air pipe at the top of the drying chamber and the inlet air at the bottom of the drying chamber .This pipe is expected to be functioning only during the off sunshine time .During day time, the bottom inlet of the drying chamber is closed and the top outlet which attached with an exist fan is opened to enable the wet air has to flow freely out of the dryer. Some of the air can be recirculated from the recirculate pipe to obtain high velocity. However, during the night, the surrounding weather is very humid .Therefore, the use of humid air at night is not suitable. The inlet from both sides of the solar collector will be closed, so that, air

from surrounding is not allowed to enter the drying chamber. The outlet at the top is also closed. Therefore, the air is trapped in the drying chamber will be recirculated. The moisture remove from the product carried out by drying air will be flowed to the desiccant material through the recirculate pipe. The moisture will be adsorbed by the desiccant. Hence, the air supply to the product will content low moisture to carry other drying procedure. This process will be repeated until the desiccant saturated. The saturated desiccant will be regenerated at day time.

D. Photovoltaic with storing batteries connected to the controlled speed fans.

A photovoltaic system is implemented in the system to generate the required power for running the fans .Two solar PV panels with total output power of around 100 watts would be enough to supply the whole system. These solar panels are placed on an adjustable rotating frame to choose the best usable inclined angle. In Melaka city, Malaysia, It is preferred to adjust the panels at 10 degree angle from the horizon to ensure that the sun radiates rays are perpendicular to the panel's surfaces [19]. Fixing the PV panels at 10 degree enable them to produce more power and then increase its efficiency. A storing battery is also used to store the excess energy during the day and supply it at night .Moreover, a controller is connected with the PV system so as to avoid an over charge of the battery and prevent it from damage.

III. MATERIALS USED IN THE SYSTEM

Table I concludes the diverse materials used for the various parts of the design and their thicknesses.

TABLE I
CHARACTERISTICS AND MATERIALS OF THE DESIGNED SYSTEM .

Part	Material	Thickness	Thermal Conductivity
Casing	Stainless steel,	2 mm	51.9 W/m·K
Solar absorber	Aluminum	2 mm	205.0 W/m·K
Transparent cover materials	Antireflective coated glass	4 mm	0.8 W/m·K
Side Insulating Materials	Silicon rubber and polystyrene	2 cm	0.03 W/m·K
Back insulation	Fiberglass wool and polystyrene	4 cm	0.08 W/m·K
Feedback pipe	Polyvinyl chloride (PVC)	4 mm	.024 W/m·K
Solar Absorber Coating	Black chrome Selective coatings	1 mm	-

The casing of the drying device is made up of stainless steel with a thickness of 2 mm. Stainless steel is preferred amongst other materials due to its possession of some features such as, its conductivity is small compared to other metals such as copper and aluminum .Moreover, it is suitable to be used in tropical zones like Malaysia due to its ability to stand in rainy seasons and resists the corrosion up to some extended limit .Above from that ,the cost of stainless steel is cheaper than other metals of the same features .

IV. SIMULATION OF THE DRYER SYSTEM

The performance of the solar dryer depends at most on the distribution of the air flow of heat throughout the body of the dryer. Optimum designing of a dryer chamber is required to obtain high value heat/mass transfer rates and regular drying process by getting rid of an undesirable aerodynamic theory in the chamber. The aim of the simulation is to figure out the path and flow of the air inside the drying chamber and then predict the necessary editions before the fabrication. CFD can generate good behavior of the tray drying model, higher goodness of dried items and regular drying at lowest costing. In addition to that, it intended to estimate a uniform air flow and heat distribution throughout the drying chamber .Besides from that, simulation is a salutary tool for optimizing the solar dryers and reducing drying time. In the literature. There is no perfect reference that focusing on the numerical solutions and simulations of air flow distribution and heat transfer in the interior zones of the solar dryers [20]. Therefore, in this paper, we concern more on the velocity and temperature behavior in the interior body .The previous studies proved that CFD simulation is a very powerful tool to provide results that close to the real conditions. In this paper, the simulation is held in 3D dimensions using Ansys 16 .The geometry is split into seven parts, glass, solar panels, side walls, right side inlet, left side inlet, bottom inlet, outlet, and interior walls as shown in Figure 5.

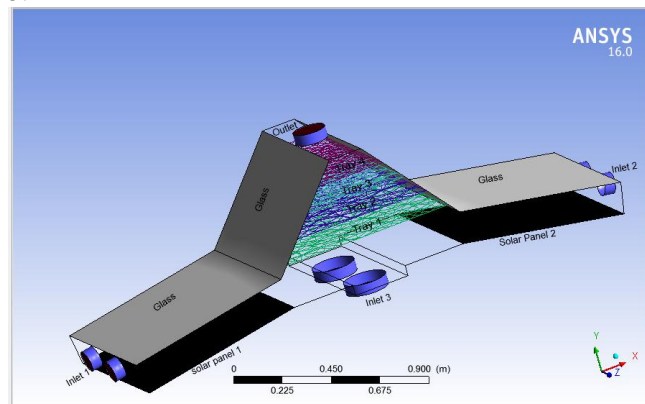


Fig. 5. The various parts of the dryer used in the simulation.

A. Computational Grid

After the geometry modeling of the design, the simulation is proceed to meshing process .in meshing, the model domain is discretized into a finite number of cells. The minimum size is (1.418 e-.003 m), the maximum face size is 0.14180 m, and the maximum size is 0.28360. It has 29029 and 6173 nodes.

B. Set up of the simulation

The inputs of the simulation are related to the normal atmospheric conditions in Malaysia, Melaka, where the ambient temperature is around 300 to 310 K at 1 atmospheric pressure. The governing equations of the simulation are energy, mass, and momentum. The fluid inside chamber is air, therefore, the flow is a turbulent and the viscosity equation is k-epsilon with enhanced wall treatment. Materials used are air as the fluid ,glass, steel ,aluminum as a solid .Regarding the radiation set

up ,it is of the discrete transfer type (DTRM).Energy iteration per radiation is 10.Maximum number of radiation iteration is 5.And the residual coverage criteria is 0.001.The model of radiation is solar ray tracing with 102 longitude and 4 latitude .

C. Boundary conditions

The simulation is assumed to be under the normal standard atmospheric conditions .The Table II below shows the details of the various boundaries with their thermal and radial conditions.

TABLE II
BOUNDARY CONDITIONS OF THE SIMULATED SYSTEM

Boundary	Type	Momentu m	Thermal Conditions	Radiation
Glass	Wall	Stationary wall	Heat flux =0	Transparent
Right side inlet	Velocity inlet	3 m/s	35 °C	Boundary temperature
Left side inlet	Velocity inlet	3 m/s	35 °C	Boundary temperature
Bottom inlet	Velocity inlet	2 m/s	40 °C	Boundary temperature
Side wall	Wall	Stationary wall	Convection with heat transfer 2 w/mk.	Opaque
Solar panels	Interior wall	Stationary wall	Convection with heat transfer 2 w/mk.	Opaque
Outlet	Pressure outlet	atmospheri c pressure	atmospheric temperature.	Boundary temperature
Interior boundary	Interior wall	Stationary wall	Alternative	Transparent .Opaque

V. RESULTS AND DISCUSSION

In this CFD simulation, the equations of Energy, Momentum, Turbulence flow, and Radiation were numerically solved. The schemes of solution and discretization and used for these equations are: Standard and First Order Upwind scheme for Momentum, Semi Empirical Pressure (SIMPLE), Turbulence Dissipation Rate and Kinetic Energy. The main Objective of this simulation is to:

1. Investigate the flow of the forced air inside the body of the dryer and then assist the uniformity of it in all loci along the dryer.
2. Evaluate the temperature profile and velocity profile along the entire body of the dryer.
3. Draw chart lines of velocity and temperature along two perpendicular imaginary lines (vertical and horizontal) and also figure out the velocity vector at inlets and outlet of the dryer.

In the first objective, three inlets are selected to present the air flow distribution inside the dryer, stream one starts from inlet 1, stream 2 starts from inlet 2, and stream 3 starts from inlet 3. Fig. 6 shows air streamlines and their behavior in the dryer.

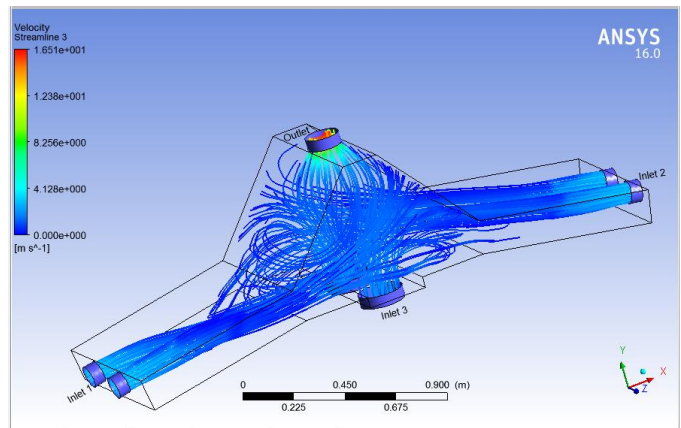


Fig. 6. Air flow streamlines starting from inlets to outlet.

It can be seen that the air is flowing to a large degree in a uniform way starting from inlet points to the outlet. From the figure, we may find that the maximum velocity speed is near to the inlet points and then it slows down gradually towards the outlet point. This is a logical result due to the existence of fixed forced fan at the inlets of the dryer. It is also visible that the air velocity in the locations close to inlet windows is higher than other locations. The high intensity of the air in the drying chamber is a desirable feature in order to remove more moisture from products. From the figure too, it is easy to see that the velocity of air streamlines ranges from 0 to 3.9 m/s except of the exit domain. The air exiting the dryer is sucked out with an exhaust fan that is the reason along with the small diameter why the velocity at the outlet records high values.

Now, to help in performing the other two objectives, we are taking some useful tools to study the temperature and velocity behavior in all directions. In this simulation, five Hypothetical planes (horizontal and vertical) along the x axis and y axis are implemented to study the temperature and velocity contours in the drying chamber. The first horizontal plane is drawn parallel to the bottom surface of the chamber and connects the two extreme edges of east and west solar panel's casing passing through all horizontal points that lie above the solar panels and the lower part of the chamber .It is positioned at 10 cm distance above the bottom surface of inlet 3. Whereas, the first vertical plane is placed at the center of the chamber and connects between the points at the surfaces of inlet 1, inlet 2, and outlet .The third plane is perpendicular to plane 2 and linked between the inlet 3 and the outlet. Finally, the remaining two planes are vertical and they positioned on a surface that joining the solar panel casing with the chamber. Fig. 7 displays all these five imaginary planes to study the temperature and velocity through them.

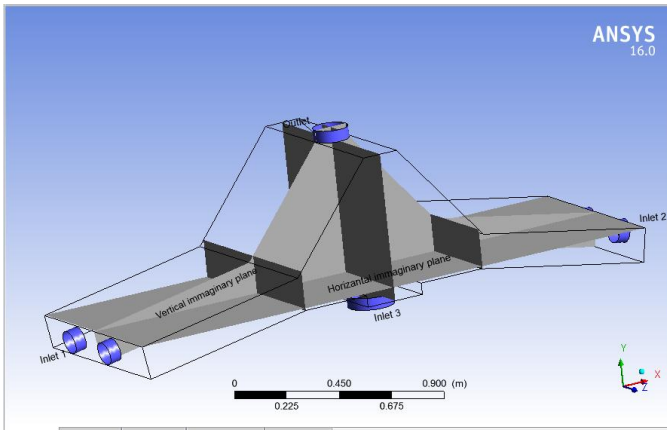


Fig. 7. Imaginary planes inside the dryer.

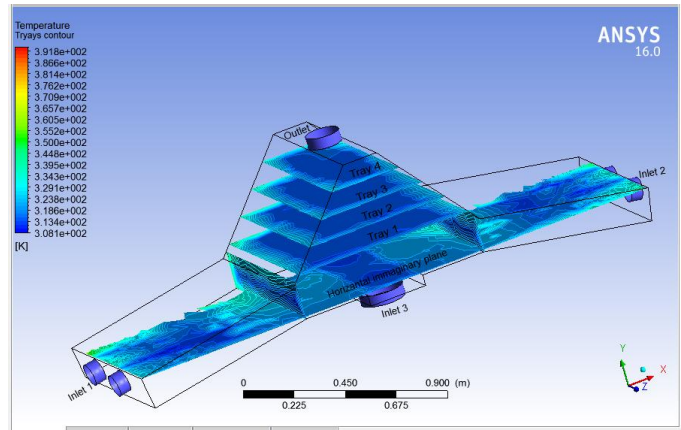


Fig. 9. Temperature profile through the horizontal planes.

For studying the temperature's profile, we are accomplishing this target in two steps. The first step is studying the temperature profile throughout the horizontal and vertical planes only, (Fig. 8). The second step is analyzing the temperature profile along the trays inside drying cell in addition to other vertical planes, Fig. 9.

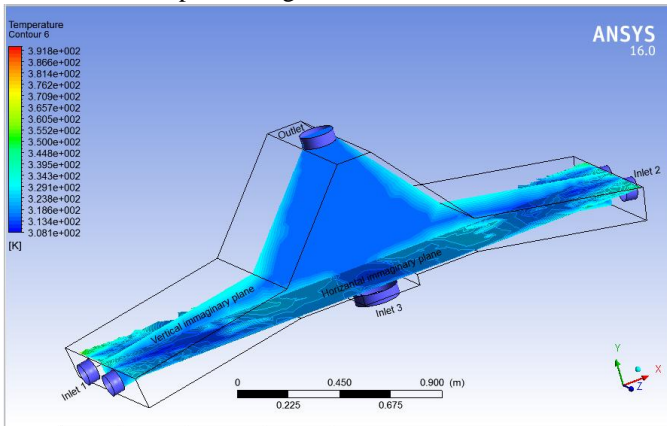


Fig. 8. Temperature profile on vertical and horizontal imaginary planes.

As it can be seen from the figure 9, the resulted temperature is alternative from one place to another. The maximum temperature given is around 354 k which is at the solar absorber plates whereas the lowest temperature is 310 k at the inlet 3. It could be observed that the temperature inside the chamber along the vertical line is lower than that on the horizontal plane. By focusing more on the solar panels area, it can be noticed that the temperature increases dramatically as long as we move away from the center of the fans towards the left or right edges. From the other side, it is noticed that the temperature at the bottom of the chamber is lower than that at the top.

On the other hand, the temperature distribution along the trays and other hypothetical planes are shown in the figure (9).

It is evident from the figure that the temperature distinct from position to another along all trays planes. It might be seen that the ends of trays towards the two solar panels achieve the highest temperature, whereas, the middle parts of all trays possess lesser temperature than that at the edges facing opposite side of solar panels. Moreover, the area of these colder edges at the left and right of the solar panels crawl gradually to the middle area as long as we move towards the top of the chamber. The maximum temperature inside the chamber is around 343 k (69.85 °C), whereas the minimum temperature is around 320 K (46.85 °C) above the inlet 3 fans.

In a same manner, the velocity distribution inside the body of the dryer was analyzed in two steps. The first one is along the horizontal and vertical hypothetical planes as shown in Fig. 10.

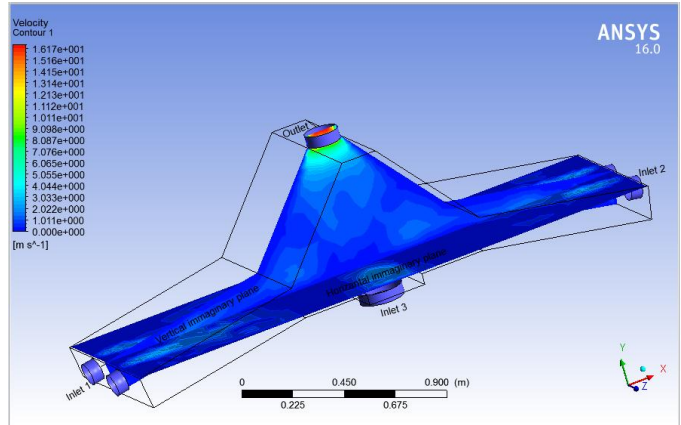


Fig. 10. Velocity profile on the horizontal and vertical imaginary planes.

It might be noticed from the figure that the velocity of the air is high at the inlets compared to the rest locations. For example, the velocity of the air entering from the inlet 1 is between 3 and 4 m/s where it decreases progressively as long as it moves further towards the chamber. Moreover, velocity along the middle zone of the vertical plane inside chamber is higher than that in the solar casings. It might be odd to see that the maximum velocity is at the outlet of the chamber, however, this increase is due to the exhaust fan located at the outlet hole.

The second step of studying the velocity contour is through trays inside the chamber as well as other vertical planes at the outlet of solar panels Fig. 11.

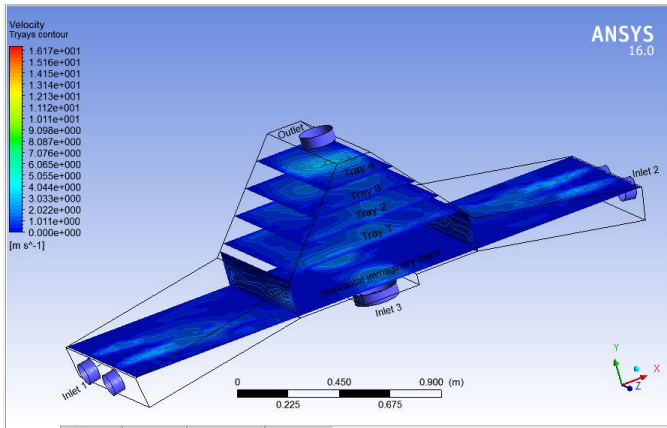


Fig. 11. V groove solar collector. Velocity profile through the horizontal and other imaginary planes.

It is clear from the figure that the velocity of air in the middle part of trays is higher than that at the edges. Unlike the temperature profile which has higher temperature of tray’s edges facing outlet of solar panels compared to middle parts, the velocity is almost same throughout the four edges of all trays. Besides that, it could be noticed that the velocity at the vertical planes at the outlet of solar panels is quite high, however it is lower than that inside the solar panel’s casings. Fig. 12 presents temperature and velocity distribution along all the imaginary planes inside the dryer body.

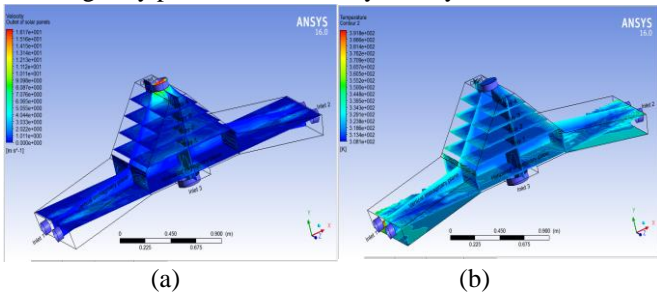


Fig. 12. (a) Temperature profile along all the imaginary planes, (b) Velocity profile along all imaginary planes.

After evaluating the results of temperature and velocity profiles, it would be beneficial if we consider and estimate the velocity vector inside the dryer. In this process, our aim is to visualize the manner of movement of air particles inside the whole dryer, specifically throughout trays.

The resulted velocity vector of the design is shown in figure Fig. 13.

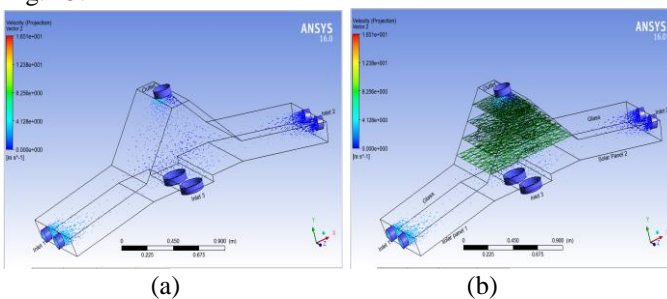


Fig. 13. Velocity vector through the dryer system: (a) without trays, (b) with trays.

The Fig. 13, (a) presents the velocity vector inside the dryer’s body regardless of trays .Whereas Fig.13 (b) shows the velocity

vector of the dryer with the consideration of the existence of the trays. These velocity vectors provide results similar to that of the velocity profiles presented in Fig. 10 and Fig. 11. Moreover, it is noticeable that numerous air particles existed inside the chamber more than other parts of dryer which is very favored and powerful feature for better drying. From the figure as well, it might be seen the positive affect of the bottom fans at inlet 3 in distributing the air throughout the chamber. The figures of velocity vectors illustrate that velocity values of air range from 0 to 4 m/s.

Now, in order to obtain the third objective of simulation mentioned above in this paper, two different lines along the X and Y axis are implemented to study as well as sketch charts of the velocity and temperature in diverse locations of the interior body of the dryer at a specific points with a constant distance from each other Fig. 14.

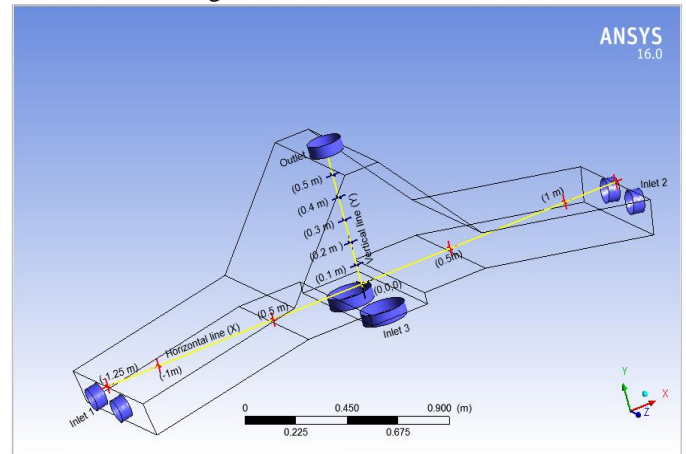


Fig. 14. The hypothetical lines along the X and Y axis.

As it can be seen from the figure above, seven points are selected along the horizontal line, two points inside each solar casing, one at each outlet of the solar casing, and the last one at the center point of drying chamber. Whereas, five points are selected through the vertical line at a constant distance of 10 cm from each other. Therefore, the next step could be proceed further is to begin with sketching the velocity graph along the X and Y axis. The resulted chart of velocity along x axis is presented in the Fig. 15.

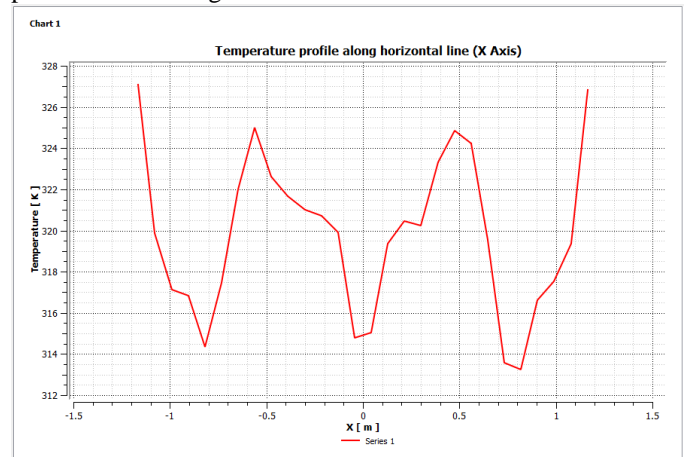


Fig. 15. Temperature variation along the X imaginary axis.

The drawn graph is semi symmetrical around the center point (0, 0, 0). The maximum temperature recorded along this axis is about 327 K (53.85 °C) at the outlet of the left and right solar casing. On the other side, the minimum temperature was recorded is about 313.5 K in the solar panel's close to the fan at inlet 2. It can be noticed that the temperature at the extreme ends of the solar casings start with a temperature of around 327 K and then decreases sharply till it reach near to 314 K at a horizontal distance of 80 cm from the center. Starting from this distance, the temperature raises quickly until it reaches close to the outlet point of solar panel. Between the two outlet points of the solar or inside the chamber, the temperature is fluctuating increase and decrease. This chart proves the same results explained in the temperature profiles in Fig. 8 and Fig. 9 that the temperature at the middle of the chamber is lower than at the four edges. On the other hand, the temperature profile follows different manner along the Y axis from that along the X axis as it can be seen in Fig. 16.

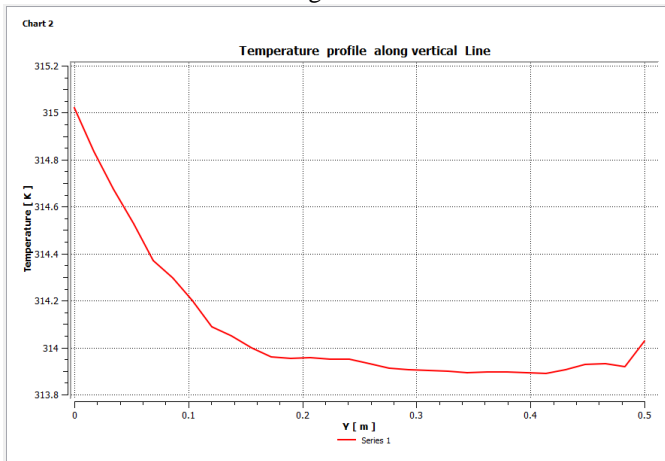


Fig. 16. Temperature variation along the Y imaginary axis.

It is clear from this figure that the temperature decreases dramatically starting from the center point at the bottom of chamber till it reach the minimum value at trays number 4 which is at a height of around 547 cm above the center point. It could be noticed as well that the temperature gets down sharply from the rest point up to second tray and then keeps with similar temperature above the tray number 3. The minimum temperature was recorded at height 47 cm above the center point with a value of around 313.9 whereas the maximum value was about 315.1 k.

Finally, we come to sketching of the velocity profile along the two hypothetical lines along the X and Y axis .Fig. 17 presents the velocity profile along the horizontal axis, X axis. It could be seen that the manner of the velocity is somehow reversed to that of temperature along the same axis. In this semi symmetrical graph, velocity from both inlets, 1 and 2 has a drastic increase begins from the inlet point until it reaches a distance of around 80 cm away from the center point. At this distance, the maximum velocity value was recorded is around 1.21 m/s .However, the velocity between points located at a horizontal distance of (80 and -80) away from the center has an opposite behavior. In this area, velocity decreases dramatically from both sides until the exit of solar casings at a distance of 50

cm from the center .After that velocity fluctuates towards the center point reaching the minimum value of around 0.1 m/s at -13 cm distance from the center of the x axis.

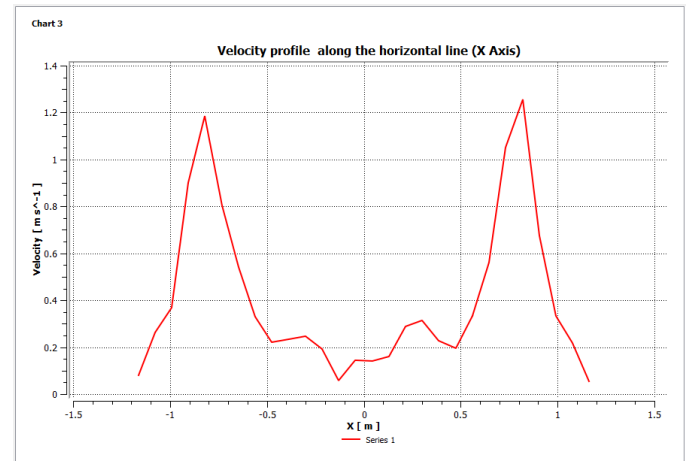


Fig. 17. Temperature variation along the Y imaginary axis.

Moreover, the velocity along the Y axis is presented in Fig. 18. There is only one pattern of behavior of this graph as it is shown in the figure below. The velocity raises up gradually starting from the center point to the highest point at the top tray in the chamber .The maximum recorded value of velocity inside chamber is around 2.3 m/s at 50 cm vertical distance from the center.

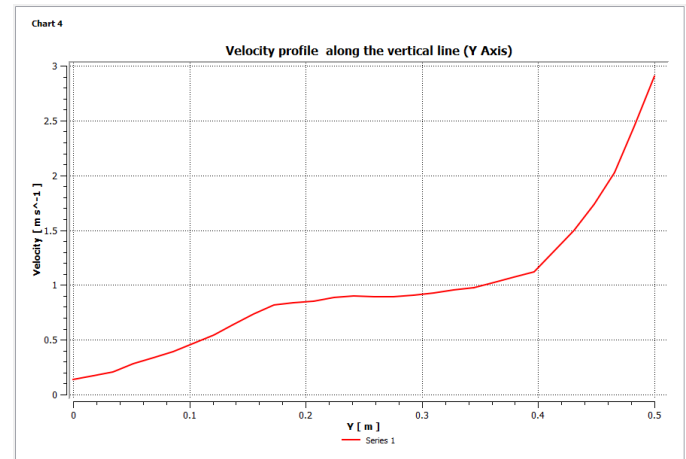


Fig. 18. Velocity variation along the Y imaginary axis.

The results of the system shows a clear improvement in terms of temperature achievement and drying capability compared to the previous dryers of the same concepts as presented in [21]. The authors there improved much regular drying of items in both of the trays is accomplished within desiccating drying .The designing integrated with a reflecting mirror to enhance the regenerating of the desiccants and measured it to dried green peas and pineapples. The beneficial thermal increment of almost 10 °C was attained with mirror, which minimized dry period by 2 hours for green peas and 4 hours for pineapples. The designed system in this paper is similar to the dryer presented in [21] according to the basic concept and function. However, more concepts and enhancement are performed in this design and they have been demonstrated. The temperature achieved in this proposed drying chamber which ranges

between 45 °C to 65 °C along with the high velocity of the air provided by the bottom fans can affect significantly in order to reduce the drying rate and increase the drying efficiency.

VI. CONCLUSION

A mixed mode solar dryer, integrated with desiccant materials has been designed and optimized. The design of the dryer possesses several features among the previous designs such as, recirculate pipe, couples solar panels, bottom fans beneath the trays of the chamber, and the arrangements of trays. Moreover, various parameters which influence critically the drying process such as airflow, temperature, and velocity profiles have been optimized and analyzed using CFD tool. The optimized results present a reasonable and an acceptable results which is close to the real conditions. From the simulation results it is profitable to conclude that:

1. The design shows a uniform air flow throughout the dryer, especially inside the chamber. This uniformity might solve the problem of drying the products at the bottom of the drying chamber faster while the upper once remain wet.
2. From this design as well it was capable to produce higher temperature inside the chamber if we neglect the bottom fans at the inlet 3 .However, it was preferred to achieve the most uniform air flow even with lower temperature. Therefore, two air blower fans are installed inside the chamber at the bottom to fulfil this purpose.
3. The highest temperature in the dryer is given as around 354 k or 80 °C which located above the solar absorber plates, whereas, and the minimum recorded temperature is 310 k. And also from temperature profiles of trays, it can be seen that the temperature on all trays is almost same. In contrast, the temperature of the middle parts of all trays is lower than that at the edges.
4. The velocity profile of trays has an obverse manner of that of the temperate profiles from the side that the middle parts in trays possess higher velocity than that at the edges. The maximum velocity is around 4 m/s near the exit of the dryer.

The simulation results indicate that the air flow as well as the heat transfer are in good agreement. In addition, the mixed mode solar dryer is the most suitable method since it should provide the highest temperature and lower drying time. The simulation results provide a valuable readings and information that can recognize the drawbacks of the system and based on this it can be assisted in further improvement of the design. Eventually, it is very advisable if the results of simulation ought to be validated with an experimental work.

REFERENCES

- [1] D. M. Parikh, "Solids Drying : Basics and Applications," *Chem. Eng.*, no. October, pp. 1–12, 2014.
- [2] O. . Ekechukwu and B. Norton, "Review of solar-energy drying systems II: an overview of solar drying technology," *Energy Convers. Manag.*, vol. 40, no. 6, pp. 615–655, 1999.
- [3] G. Boyle, "Power for a Sustainable Future EPUB By Godfrey Boyle," *Oxford Univ. Press*, p. 566, 2012.
- [4] A. Bakhshipour, A. Jafari, and A. Zomorodian, "Vision based features in moisture content measurement during raisin production," *World Appl. Sci. J.*, vol. 17, no. 7, pp. 860–869, 2012.
- [5] A. A. Zomorodian and M. Dadashzadeh, "Indirect and Mixed Mode Solar Drying Mathematical Models," *J. Agr. Sci. Tech.*, vol. 11, pp. 391–400, 2009.
- [6] C. L. Hii, C. L. Law, M. Cloke, and S. Suzannah, "Thin layer drying kinetics of cocoa and dried product quality," *Biosyst. Eng.*, vol. 102, no. 2, pp. 153–161, 2009.
- [7] <https://www.agmcontainer.com/blog/desiccant/selecting-desiccant/>, "Selecting the Right Desiccant." .
- [8] I. N. Simate, "Optimization of mixed-mode and indirect-mode natural convection solar dryers," *Renew. Energy*, vol. 28, no. 3, pp. 435–453, 2003.
- [9] E. Mathioulakis, V. T. Karathanos, and V. G. Belessiotis, "Simulation of air movement in a dryer by computational fluid dynamics: Application for the drying of fruits," *J. Food Eng.*, vol. 36, no. 2, pp. 183–200, 1998.
- [10] D. P. Margaris and A. G. Ghiaus, "Dried product quality improvement by air flow manipulation in tray dryers," *J. Food Eng.*, vol. 75, no. 4, pp. 542–550, 2006.
- [11] J. Smolka, A. J. Nowak, and D. Rybarz, "Improved 3-D temperature uniformity in a laboratory drying oven based on experimentally validated CFD computations," *J. Food Eng.*, vol. 97, no. 3, pp. 373–383, 2010.
- [12] K. Kant, A. Shukla, A. Sharma, A. Kumar, and A. Jain, "Thermal energy storage based solar drying systems: A review," *Innov. Food Sci. Emerg. Technol.*, vol. 34, no. September, pp. 86–99, 2016.
- [13] O. Saadatian, K. Sopian, B. R. Elhab, M. H. Ruslan, and N. Asim, "Optimal Solar Panels ' Tilt Angles and Orientations in Kuala Lumpur , Malaysia," *Adv. Environ. Biotechnol. Biomed.*, pp. 100–106, 2013.
- [14] O. S. Idowu, O. M. Olarenwaju, and O. I. Ifedayo, "Determination of optimum tilt angles for solar collectors in low-latitude tropical region," *Int. J.*, vol. 4, no. 1, p. 29, 2013.
- [15] F. Akarslan, "Solar-Energy Drying Systems," *Model. Optim. Renew. Energy Syst.*, pp. 1–21, 2012.
- [16] T. Bombay, "A review on indirect solar dryers," vol. 10, no. May 2015, pp. 3360–3371, 2016.
- [17] S. Misha, S. Mat, M. H. Ruslan, K. Sopian, and E. Salleh, "Review on the application of a tray dryer system for agricultural products," *World Appl. Sci. J.*, vol. 22, no. 3, pp. 424–433, 2013.
- [18] S. Misha, S. Mat, M. H. Ruslan, and K. Sopian, "Review of solid/liquid desiccant in the drying applications and its regeneration methods," *Renew. Sustain. Energy Rev.*, vol. 16, no. 7, pp. 4686–4707, 2012.
- [19] B. R. Elhab *et al.*, "Optimizing tilt angles and orientations of solar panels for Kuala Lumpur, Malaysia," *Sci. Res. Essays*, vol. 7, no. 42, pp. 3758–3767, 2012.
- [20] Y. M. Yunus and H. H. Al-Kayiem, "Simulation of Hybrid Solar Dryer," *IOP Conf. Ser. Earth Environ. Sci.*, vol. 16, p. 10, 2013.
- [21] V. Shanmugam and E. Natarajan, "Experimental study of regenerative desiccant integrated solar dryer with and without reflective mirror," *Appl. Therm. Eng.*, vol. 27, no. 8–9, pp. 1543–1551, 2007.